Electronic Supplementary Information

Prior Oxidation of Ni Substrate Increases Number of Active Sites in Ni_3S_2 Obtained by Sulfidation and Enhances Its Multifunctional Electrocatalytic Activity

Anantharaj Sengeni[1,2,3]* and Suguru Noda[2,3]

[1.] Laboratory for Electrocatalysis and Energy, Department of Chemistry, Indian Institute of Technology, Kanpur 208 016, Uttar Pradesh, India

[2.] Department of Applied Chemistry, School of Advanced Science and Engineering, Waseda University, 3-4-1 Okubo, Shinjuku-ku, Tokyo 169-8555, Japan

[3.] Waseda Research Institute for Science and Engineering, Waseda University, 3-4-1 Okubo, Shinjuku-ku, Tokyo 169-8555, Japan

* Correspondence should be addressed to: *ananths@iitk.ac.in*, and *anantharajsengeni@gmail.com*

Determination of loading of Ni_3S_2-O/Ni:

The mass loading of a catalyst grown on a substrate is calculated using the formula given below.

Loading of Ni_3S_2-O/Ni

= increase in mass as $Ni_3S_2 \times MW_{NiS2/3}/(MW_{NiS2/3}–MW_{Ni})$

+ increase in mass as $Ni(OH)_2 \times MW_{Ni(OH)2}/(MW_{Ni(OH)2}–MW_{Ni})$

Please note that though the catalyst is identified as Ni_3S_2-O/Ni, the 'O' in the same stands for $Ni(OH)_2$ resulted from the peroxidation of the substrate. From the Ni $2p_{3/2}$ XPS spectrum (Figure 3a), we could see that the two deconvoluted Ni^{2+} peaks (assigned to NiO and $Ni(OH)_2$) are having almost the same area under the peak and Ni^{2+} assigned to NiO could also be assigned to Ni^{2+} in Ni_3S_2. Hence, we can assume that the half of surface Ni is in Ni_3S_2 while the remaining half is in $Ni(OH)_2$. Since the mass increase via conversion of 1 mol Ni to 1 mol Ni_3S_2 is 21.4 g ($Ni+2/3S \rightarrow 1/3Ni_3S_2$) and that to 1 mol $Ni(OH)_2$ is 34.0 g ($Ni+2OH \rightarrow Ni(OH)_2$), it is attributed that 21.4/(21.4+34.0)x100% = 38.6% of the measured increase in weight to Ni_3S_2 and 34.0/(21.4+34.0)x100% = 61.4% of the measured increase in weight to $Ni(OH)_2$ and calculated the total mass of Ni_3S_2-O on Ni to be ~0.6 mg cm^{-2} as follows.

Total increase in weight after 100 s of anodization = 0.181 mg cm^{-2}

38.6% of total increase in weight corresponding to Ni_3S_2 in Ni_3S_2-O on Ni = 0.070 mg cm^{-2}

61.4% of total increase in weight corresponding to $Ni(OH)_2$ in Ni_3S_2-O on Ni = 0.111 mg cm^{-2}

Hence,

Loading of Ni_3S_2 in Ni_3S_2-O on Ni

$$= 0.070 \text{ mg cm}^{-2} \times ((240.2 \text{ g mol}^{-1}/3)/(21.4 \text{ g mol}^{-1}) = 0.262 \text{ mg cm}^{-2}$$

Loading of $Ni(OH)_2$ in Ni_3S_2-O on Ni

$$= 0.111 \text{ mg cm}^{-2} \times (92.7 \text{ g mol}^{-1})/(34.0 \text{ g mol}^{-1}) = 0.303 \text{ mg cm}^{-2}$$

Hence, the total loading of Ni_3S_2-O on Ni

= 0.262 mg cm^{-2} + 0.303 mg cm^{-2} = 0.565 mg cm^{-2} ≈ **0.6 mg cm^{-2}**

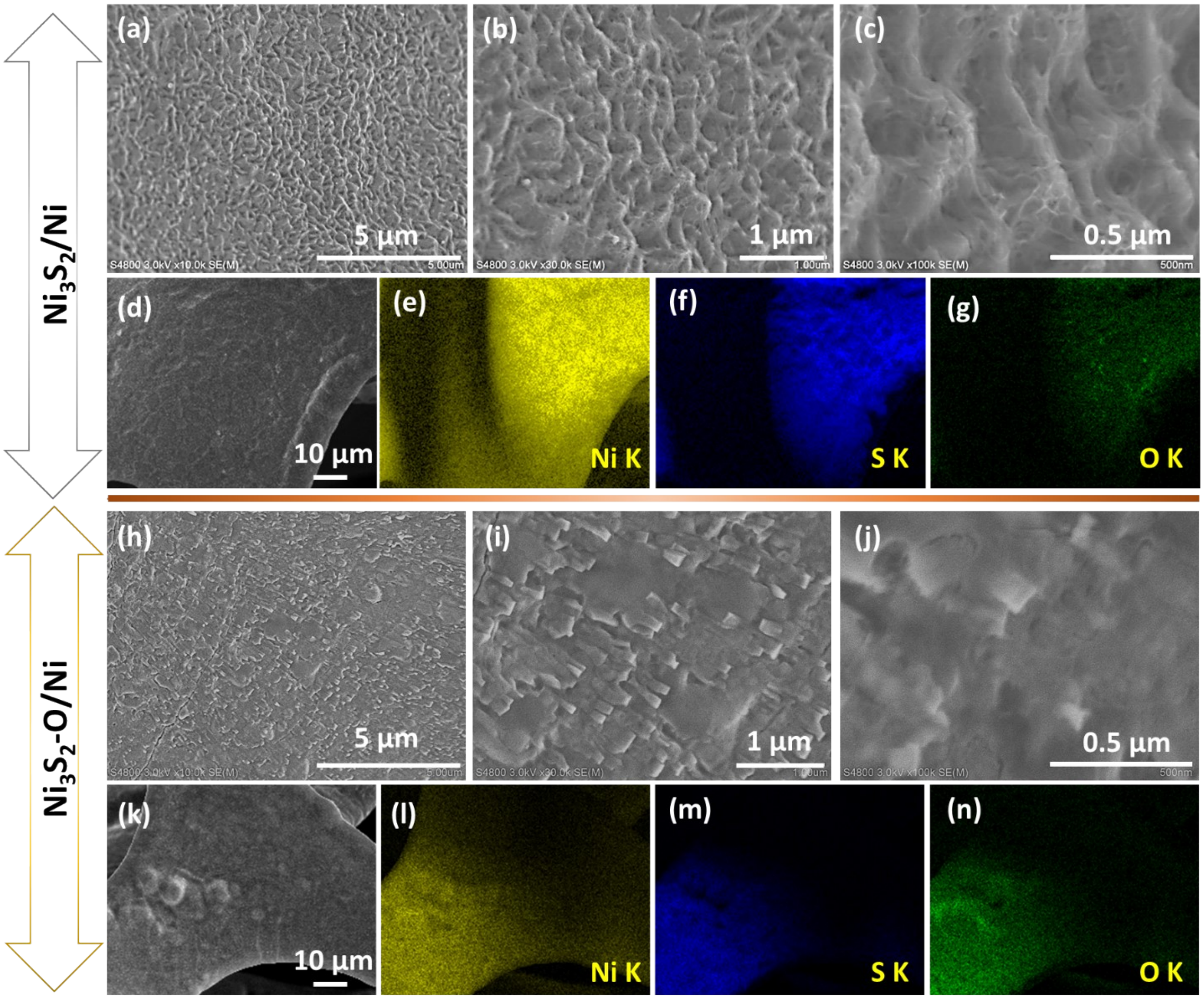

Figure S1: (a-c) SEM micrographs of Ni_3S_2/Ni with increasing magnifications. (d) Low-magnification SEM micrograph illustrating the position of Ni_3S_2/Ni where the elemental EDS mapping was conducted for Ni (e), S (f), and O (g). (h-n) A similar set of SEM micrographs, low-magnification SEM micrograph showing the position of Ni_3S_2–O/Ni where elemental EDS mapping for the same set of elements was performed for Ni_3S_2–O/Ni, and the corresponding elemental maps in the same order.

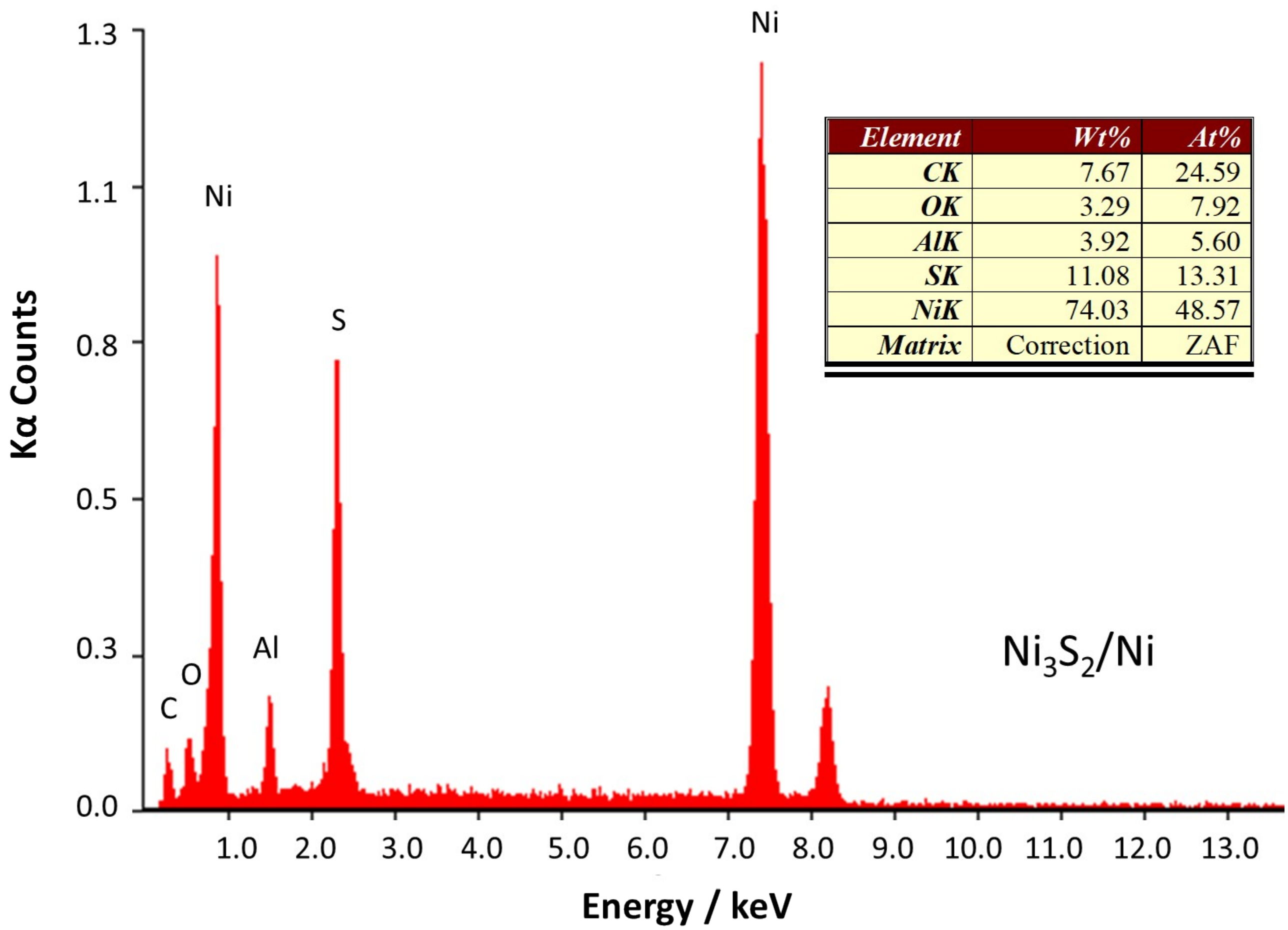

Element	*Wt%*	*At%*
CK	7.67	24.59
OK	3.29	7.92
AlK	3.92	5.60
SK	11.08	13.31
NiK	74.03	48.57
Matrix	Correction	ZAF

Figure S2: Energy dispersive X-ray spectrum of Ni_3S_2/Ni with the elemental composition in the table given as inset.

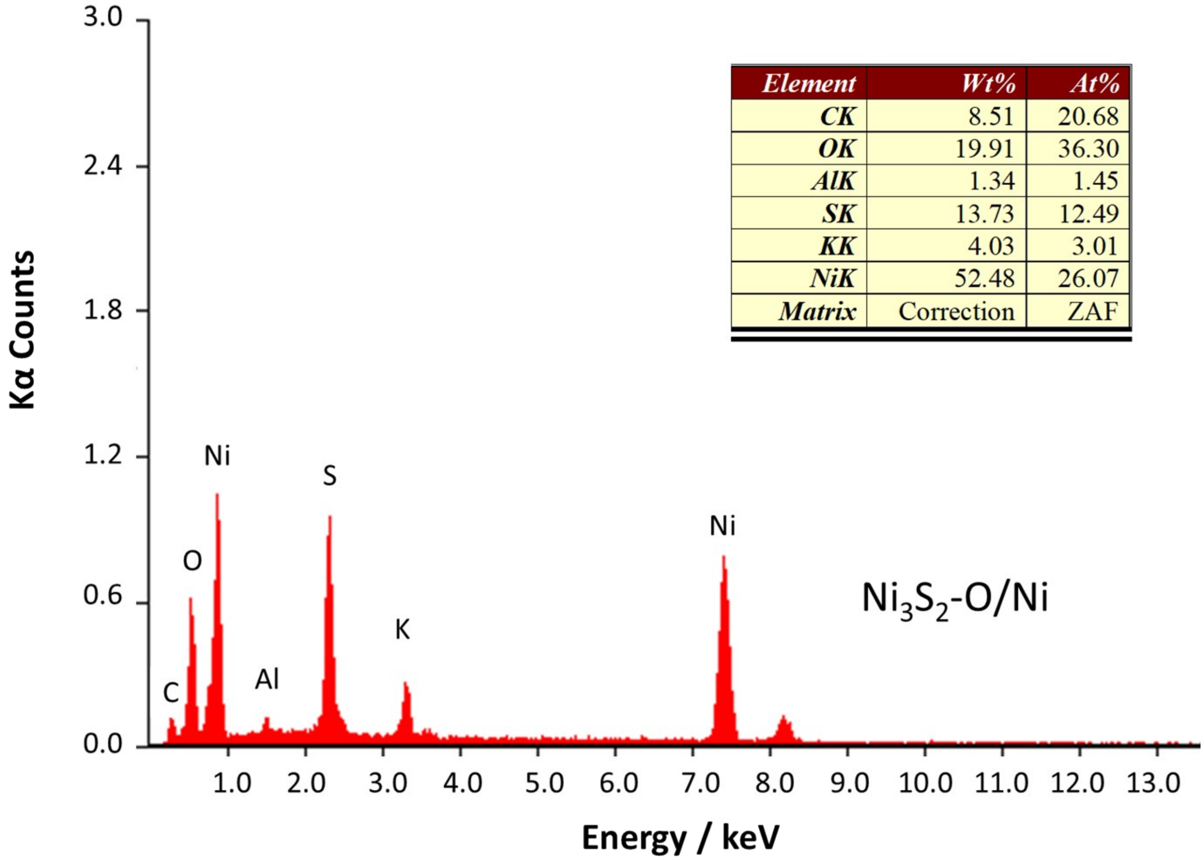

Element	*Wt%*	*At%*
CK	8.51	20.68
OK	19.91	36.30
AlK	1.34	1.45
SK	13.73	12.49
KK	4.03	3.01
NiK	52.48	26.07
Matrix	Correction	ZAF

Figure S3: Energy dispersive X-ray spectrum of Ni_3S_2-O/Ni with the elemental composition in the table given as inset.

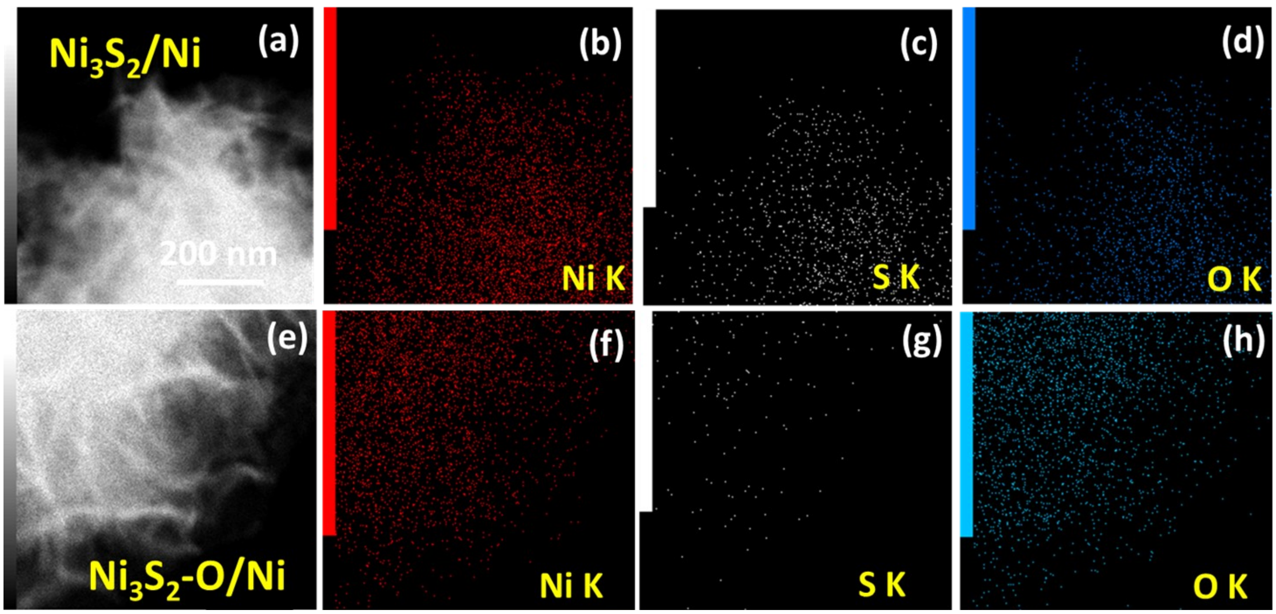

Figure S4: (a-d) STEM-HAADF image of Ni_3S_2/Ni with EDS elemental mapping of Ni (b), S (c), and O (d), respectively. (e-h) A similar set of STEM-HAADF image and elemental maps for the same elements in Ni_3S_2-O/Ni.

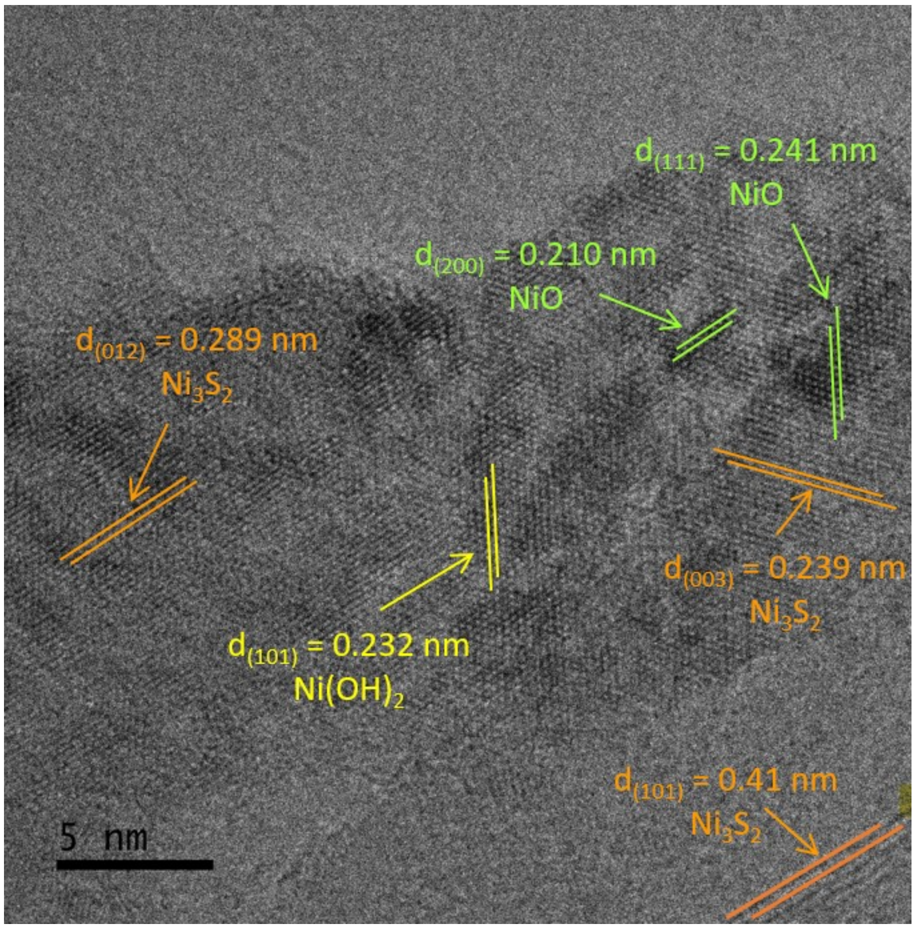

Figure S5: HRTEM image of Ni_3S_2-O/Ni showing the lattice planes of Ni_3S_2, NiO, and $Ni(OH)_2$ planes adjacent to one another.

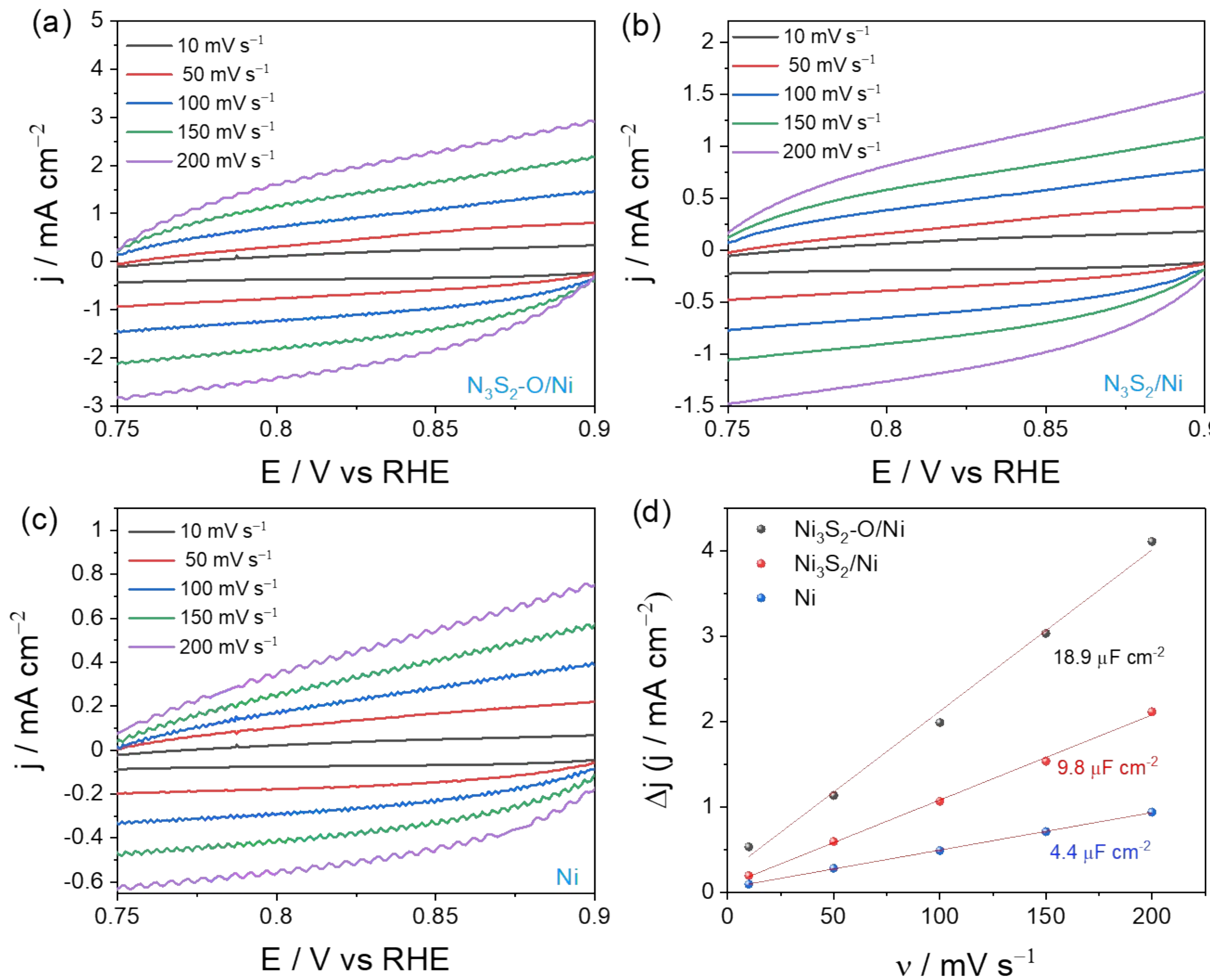

Figure S6: CVs of Ni foam and Ni_3S_2-O/Ni in 1.0 M KOH with increasing scan rate in a non-Faradaic region. (c) Plot of difference in the double-layer charging current against scan rates.

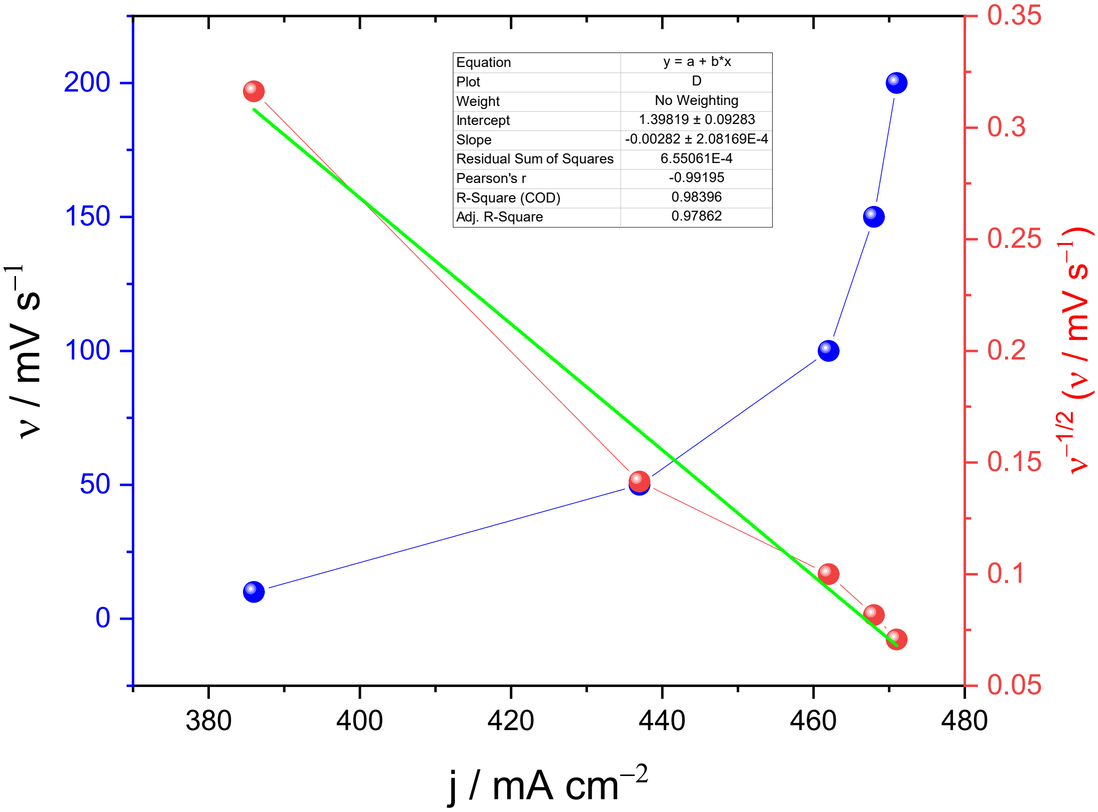

Figure S7: Plot of scan rate (blue) and inverse of the square root of the scan rate vs the MOR current density of Ni_3S_2-O/Ni in 1.0 M KOH containing 0.5 M methanol at the anodic vertex potential (1.724 V vs RHE).

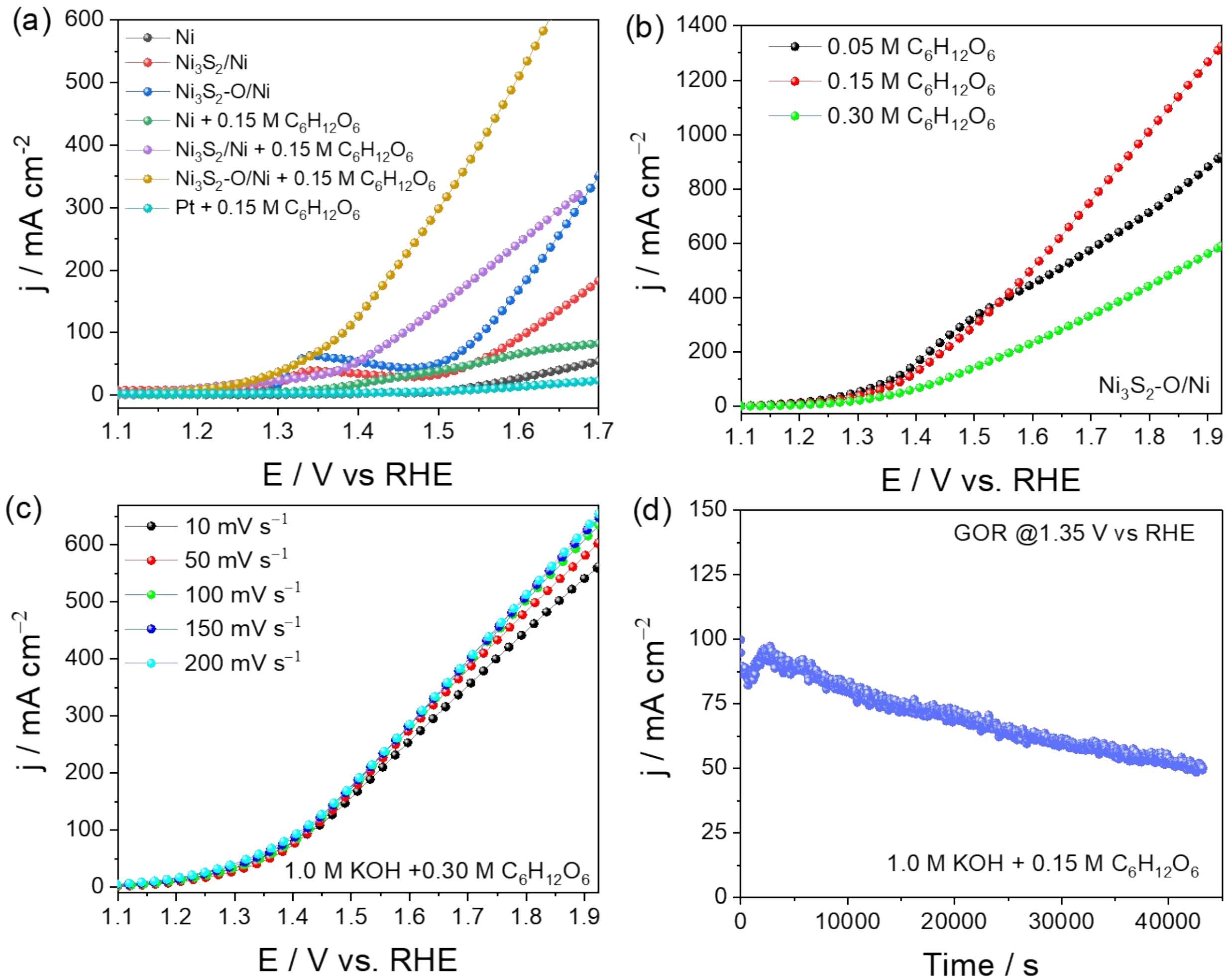

Figure S8: (a) GOR LSVs of Ni_3S_2–O/Ni and Ni foam in 1.0 M KOH containing 0.15 M glucose recorded at 10 mV s^{-1} in comparison with the LSVs obtained only in 1.0 M KOH. (b) GOR LSVs of Ni_3S_2–O/Ni showing the concentration effect. (c) GOR LSVs of Ni_3S_2–O/Ni showing the scan rate effect. (d) CA response of Ni_3S_2–O/Ni at 1.35 V vs RHE in 1.0 M KOH containing 0.15 M glucose.

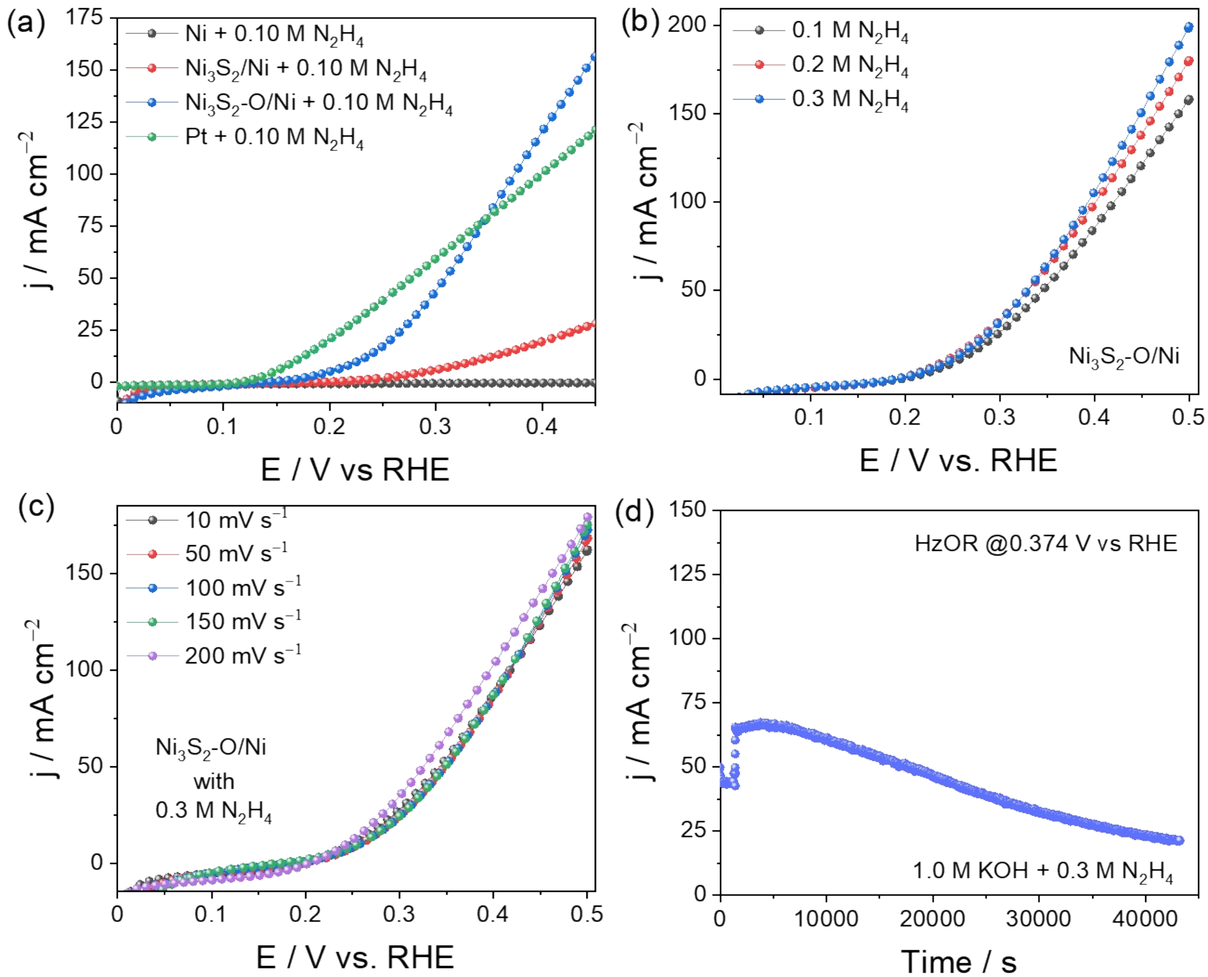

Figure S9: (a) HzOR LSVs of Ni_3S_2–O/Ni and Ni foam in 1.0 M KOH containing 0.10 M hydrazine obtained at 10 mV s^{-1} and provided in comparison with the LSVs obtained only in 1.0 M KOH solution. (b) HzOR LSVs of Ni_3S_2–O/Ni showing the concentration effect. (c) HzOR LSVs of Ni_3S_2–O/Ni showing the scan rate effect. (d) CA response of Ni_3S_2–O/Ni at 0.374 V vs RHE in 1.0 M KOH containing 0.10 M hydrazine.

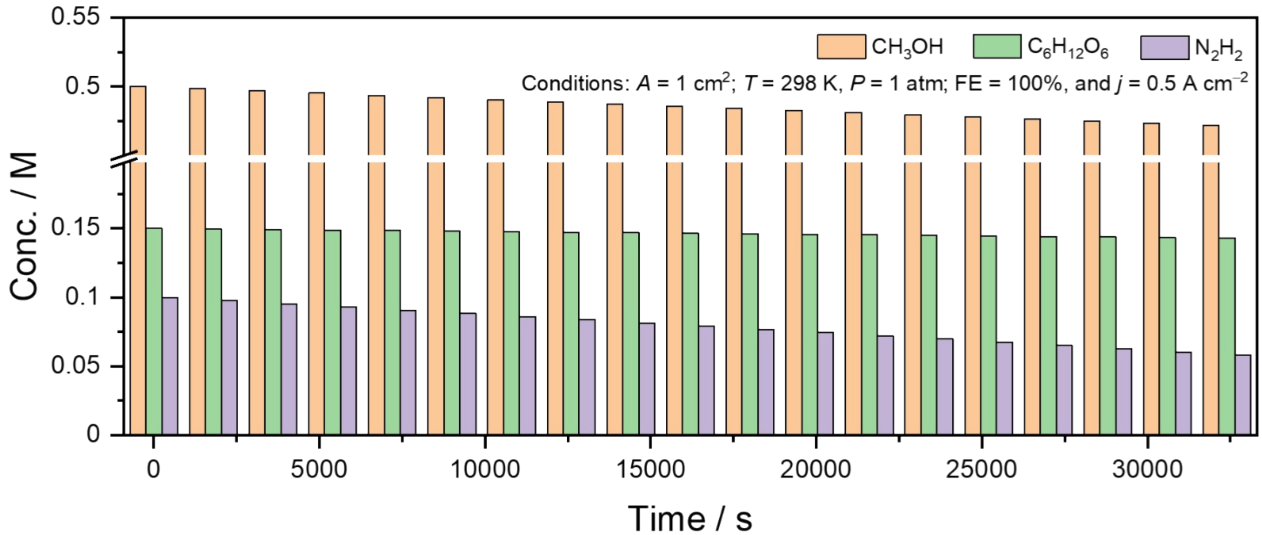

Figure S10: Calculated trend of change in concentrations of methanol (saffron), glucose (green), and hydrazine (purple) over time at prescribed conditions.